ANALYSIS OF A NONLINEAR TUNED MASS DAMPER BY USING THE MULTI-SCALE METHOD[1]

JUNFENG LIU, JI YAO, KUN HUANG, QING ZHANG, LI ZE

Faculty of Civil Engineering and Mechanics, Kunming University of Science and Technology, Kunming, China
Corresponding author Ji Yao, e-mail: 105434620@qq.com

A tuned mass damper is a kind of vibration damping device which has been widely used in tall buildings, machinery, bridges, aerospace engineering and other fields. In practical engineering applications, due to large deformation caused by large displacement, errors in engineering constructions and the existence of limit devices, the structure and tuned mass dampers inevitably produce some nonlinear characteristics, but these nonlinearities are often ignored. The results of this study confirm that the nonlinearity of the structure and the mass damper should be considered in the process of optimal frequency design, otherwise there will be a large deviation between the design optimal frequency of the mass damper and the actual optimal frequency. In this paper, nonlinear characteristics of the tuned mass damper and the main structure are considered. The first-order differential equations are obtained by using the complex average method, and the nonlinear equations of the tuned mass damper system are derived by using the multi-scale method. On this basis, the parameters are determined. The numerical results show that the error of the approximate solution method is small in the given example. The nonlinear tuned mass damper with nonlinear design exhibits a better control performance.

Keywords: nonlinear characteristics, complex average method, multi-scale method, nonlinear design, control performance

1. Introduction

Modern structures require more and more vibration reduction. This has led to the production of shock absorbers with better damping performance and lower cost so as to reduce the weight of the structure and thus improve practicality. This trend has led to the development of smaller, lighter and cheaper shock absorbers. As a result, modern structures have to face with more complex interferences and low structure weight, which often leads to nonlinear vibration. The problem of nonlinear vibration is increasingly prominent. Reduction of the nonlinear vibration becomes a significant challenge. At the same time, the design, selection and parameters of control devices become a significant research topic (Housner *et al.*, 1997; Ramlan *et al.*, 2010; Lin *et al.*, 2015; Lu *et al.*, 2018).

Passive control devices are simple to install, independent of power and cost, and have been widely studied and applied. The tuned mass damper (TMD) is a common passive control device. The principle is roughly that the energy of the main structure is transferred to the tuned mass damper through a linear or nonlinear spring, and then the energy is dissipated through the damping member connecting the main structure and the mass block. TMDs were first proposed by Watts in 1883 and subsequently patented by Frahm (1911), which aroused interest among engineers and vibration researchers. With the passage of time, Ormondroyd and Den Hartog (1928) studied an undamped primary structure and a two degree of freedom structure with

---

TMD and deduced the solution formula. Based on the above system, Den Hartog (1956) found the optimization formula based on fixed point theory in his work, which made the research of TMD more in-depth and of engineering practical significance. Subsequently, Tsai and Lin (1993) presented the analytical formula for optimal parameter design of TMD with the main structure based on Den Hartog fixed point theory. With the in-depth exploration of problems related to TMDd, studies on parameter design of linear TMD have been well made and summarized in literature (Frahm, 1911; Ormondroyd and Den Hartog, 1928; Den Hartog, 1956; Tsai and Lin, 1993; Elias and Matsagar, 2017; Warburton and Ayorinde, 1980). A mature research on linear mass dampers and an in-depth study of multiple tuned mass dampers are given in (Bhowmik and Debnath, 2022; Li *et al.*, 2020; Zhang *et al.*, 2022; Matin *et al.*, 2020; Kim and Lee, 2020), on nonlinear mass dampers in (Farshi and Assadi, 2011; Badamchi *et al.*, 2921; Alexander and Schilder, 2009) and on other mass dampers in (Qiu *et al.*, 2018; Tai, 2020; Lian *et al.*, 2018; Zhao *et al.*, 2020; Almazán *et al.*, 2007; Kecik and Mitura, 2020). It was shown that nonlinear mass dampers have longer bandwidth and vibration reduction effects. It is proved that it is effective in broadening the effective suppression bandwidth of the frequency response curve. In general, the method of introducing nonlinear stiffness into a mass damper system is to introduce stiffness nonlinearity. A more effective nonlinear stiffness is cubic stiffness. Due to the strong amplification effect of higher order terms, it brings the risk of large error, so few people have carried out an in-depth research. The Nonlinear Tuned Mass Damper (NTMD), which possesses nonlinear springs or nonlinear damping, was engineered in 1952. To solve the limitations of TMD, Robertson (1952) first studied the undamped cubic nonlinear mass damper system. The results showed that its bandwidth was much wider than TMD in the case of parameter optimization. Natsiavas (1992) studied the steady-state solution and stability of a weakly nonlinear mass damper system, and obtained the steady-state solution by using the approximate solution. In fact, the nonlinearity is inevitable, and some of its effects on the structure are so small that they can be ignored. In some cases, nonlinear factors affect the vibration process, and even lead to destruction of the material, so it is necessary to consider the influence of nonlinear factors on the structure. In the determination of mass damper parameters, the results of this study confirm that the desired damping effect can not be obtained without considering the nonlinearity of the structure. Especially when the structural nonlinearity and the mass damper nonlinearity exist at the same time, these two nonlinearities need to be considered simultaneously, otherwise the optimal design frequency will deviate greatly from the actual optimal frequency. In 2003, considering that the averaging method and the multi-scale method are not directly applicable to the research of a nonlinear mass damper system, Jiang *et al.* (2003) proposed a new method based on a complex variable averaging method in order to better distinguish the fast variable term and slow variable term in the response. The results of this method were verified by an experimental method, and it was found that it had high accuracy. Subsequently, Manevitch *et al.* (2007) adopted the complex variable averaging method and the multi-scale method to analyze the mass damper system with cubic nonlinear stiffness and verified its effectiveness by numerical solution. Subsequently, Li and Zhang (2020) obtained first-order differential equations based on the average method of complex variables, and then obtained optimal parameters of mass dampers by using the multi-scale method.

Mass dampers have many applications in building structures and automobile vibration reduction. In order to facilitate the research, the current analysis is mainly focused on an illustrative model structure with two degrees of freedom. The research on the conversion from a multi-degree of freedom main structure to a single degree of freedom system is mainly to conduct modal analysis on the main structure. Taking its first-order modal mass, the first-order frequency and first-order damping ratio, the multi-degree of freedom main structure can be approximately simplified to a single degree of freedom structure. In this paper, for the NTMD system for a two degree of freedom structure, the first order differential equations of amplitude and phase are

obtained by using the variable parameter method and average method to solve the nonlinear system. Then, the nonlinear equations of amplitude are obtained by the using multi-scale method. The accuracy of the solution process is verified by a numerical method. Finally, according to the obtained expression, the frequency parameters of the tuned mass damper are found.

2. Analysis of nonlinear TMD structure

2.1. Governing equations

According to the literature (Banerjee *et al.*, 2022), a multi-degree of freedom building structure can be idealized into a linear single degree of freedom system. When using this method for simplification, the first-order modal mass, first-order modal stiffness and first-order modal damping of the multi-degree of freedom structure can be simplified as the main structural model, and TMD is added to it. Therefore, the above structure is simplified into a two degree of freedom TMD system. In this paper, it is considered that the weak nonlinear stiffness of the structure is an inevitable parameter, so the cubic stiffness nonlinearity of the main structure and the TMD are considered.
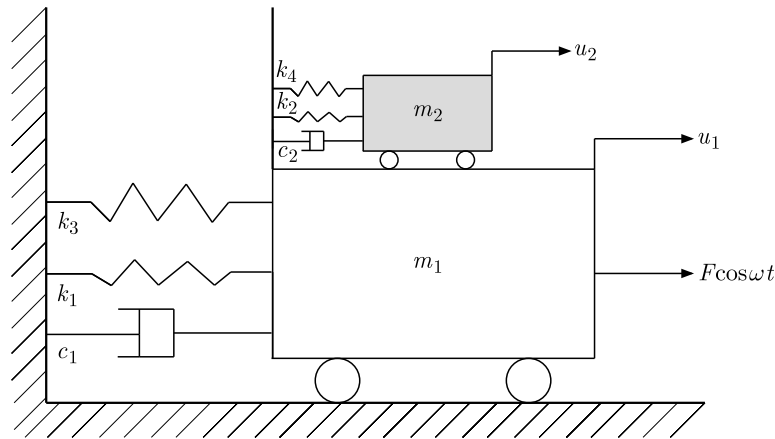

Fig. 1. Nonlinear mass dampers and structural dynamic system

Figure 1, as an illustrative example of a nonlinear mass damper system, is a two-DOF dynamic system. The main structure is influenced by a cosine harmonic excitation force with the amplitude F and excitation frequency ω. It is connected to the wall through a nonlinear spring and linear damping, and at the same time, it is connected to the mass damper through the nonlinear spring and linear damping. This model ignores frictional forces everywhere, and two coupled second-order differential equations can be obtained by Newton's second law as follows

$$
\begin{aligned}
&m_1\ddot{u}_1 + c_1\dot{u}_1 + k_1 u_1 + k_3 u_1^3 + m_2\ddot{u}_2 = F\cos\omega t \\
&m_2\ddot{u}_2 + c_2(\ddot{u}_2 - \ddot{u}_1) + k_2(u_2 - u_1) + k_4(u_2 - u_1)^3 = 0
\end{aligned}
\tag{2.1}
$$

Equations (2.1) can be written in the following form for subsequent analysis. For the derivation process one can refer to the literature (Li and Zhang, 2020)

$$
\begin{aligned}
&\ddot{u}_1 + \varepsilon\lambda_1\dot{u}_1 + \omega_1^2 u_1 + \varepsilon\alpha_1\omega_1^2 u_1^3 + \varepsilon\ddot{u}_2 = \varepsilon f\cos\omega t \\
&\ddot{u}_2 + \lambda_2(\dot{u}_2 - \dot{u}_1) + \omega_2^2(u_2 - u_1) + \alpha_2\omega_2^2(u_2 - u_1)^3 = 0
\end{aligned}
\tag{2.2}
$$

Among them

$$\frac{m_2}{m_1} = \varepsilon \qquad \frac{k_1}{m_1} = \omega_1^2 \qquad \frac{k_2}{m_2} = \omega_2^2 \qquad \frac{c_1}{m_1} = \varepsilon\lambda_1$$

$$\frac{F}{m_1} = \varepsilon f \qquad \frac{c_2}{m_2} = \lambda_2 \qquad \frac{k_3}{k_1} = \varepsilon\alpha_1 \qquad \frac{k_4}{k_2} = \alpha_2$$

By performing the coordinate transformation, converting u_1 and u_2 to new coordinates x and y, respectively, as shown below

$$x = u_1 + \varepsilon u_2 \qquad y = u_1 - u_2 \tag{2.3}$$

u_1 and u_2 can be represented in terms of x and y as follows

$$u_1 = \frac{x + \varepsilon y}{1 + \varepsilon} \qquad u_2 = \frac{x - y}{1 + \varepsilon} \tag{2.4}$$

Equation (2.4) is now represented by the new coordinates.

Substitute the expression into Eqs. (2.2) to obtain the coordinate transformed equation

$$\ddot{x} + \frac{\varepsilon\lambda_1(\dot{x} + \varepsilon\dot{y})}{1 + \varepsilon} + \omega_1^2\frac{x + \varepsilon y}{1 + \varepsilon} + \varepsilon\alpha_1\omega_1^2\frac{(x + \varepsilon y)^3}{1 + \varepsilon} = \varepsilon f \cos\omega t$$

$$\ddot{y} - \ddot{x} + \lambda_2(1 + \varepsilon)\dot{y} + \omega_2^2(1 + \varepsilon)y + \alpha_2\omega_2^2(1 + \varepsilon)y^3 = 0 \tag{2.5}$$

Equations (2.5) are generalized coordinate equations after transformation.

2.2. Taylor expansion

In order to facilitate the use of the later perturbation analysis method, Eqs. (2.5) are decoupled by using the Taylor expansion. Consider Eqs. (2.5) in terms of the mass ratio ε, expand at $r(0 + \varepsilon)$ and keep to the first term. Since ε is small, the first-order expansion can satisfy the subsequent analysis

$$r(\varepsilon) = r(0) + \varepsilon r'(0) \tag{2.6}$$

Then $r(0)$ and $r'(0)$ of Eqs. (2.5) are as follows

$$r(0) = \ddot{x} + \omega_1^2 x \qquad r'(0) = \lambda_1\dot{x} + \omega_1^2 y - \omega_1^2 x + \alpha_1\omega_1^2 x^3 - f\cos\omega t \tag{2.7}$$

and

$$r(0) = \ddot{y} - \ddot{x} + \lambda_2\dot{y} + \omega_2^2 y + \alpha_2\omega_2^2 y^3 \qquad r'(0) = \lambda_2\dot{y} + \omega_2^2 y + \alpha_2\omega_2^2 y^3 \tag{2.8}$$

From equations (2.6) to (2.8), the following decoupled equation can be obtained

$$\ddot{x} + \omega_1^2 x + \varepsilon(\lambda_1\dot{x} + \omega_1^2 y - \omega_1^2 x + \alpha_1\omega_1^2 x^3 - f\cos\omega t) = 0$$

$$\ddot{y} + \omega_1^2 y + \lambda_2\dot{y} + \alpha_2\omega_2^2 y^3 + \omega_1^2(x - y) + \omega_2^2 y$$

$$+ \varepsilon(\lambda_2\dot{y} + \omega_2^2 y + \alpha_2\omega_2^2 y^3 + \lambda_1\dot{x} + \omega_1^2 y - \omega_1^2 x + \alpha_1\omega_1^2 x^3 - f\cos\omega t) = 0 \tag{2.9}$$

The solutions of x and y can be set in the form of (2.10), where A_1 and A_2 are the expressions of complex variables of the amplitude and phase respectively, and cc is the complex conjugate of the preceding term

$$x = \frac{1}{2i\omega}A_1 e^{i\omega t} + cc \qquad y = \frac{1}{2i\omega}A_2 e^{i\omega t} + cc \tag{2.10}$$

By taking the derivatives of equations (2.10) with respect to time t, and making A_1 and A_2 functions of time t, $\dot{x}$ and $\dot{y}$ have the same features as x and y. A part of the theory refers to the equalization method in (Nayfeh and Mook, 1981)

$$\dot{x} = \frac{1}{2}A_1 e^{i\omega t} + cc \qquad \dot{y} = \frac{1}{2}A_2 e^{i\omega t} + cc \qquad (2.11)$$

Similarly, take two derivatives of equations (2.10) with respect to time t

$$\ddot{x} = A_1 e^{i\omega t} + \frac{1}{2}i\omega A_1 e^{i\omega t} + cc \qquad \ddot{y} = A_2 e^{i\omega t} + \frac{1}{2}i\omega A_2 e^{i\omega t} + cc \qquad (2.12)$$

By substituting the expressions of x, y, $\dot{x}$, $\dot{y}$, $\ddot{x}$, $\ddot{y}$ obtained by the parameter variational method and the averaging method into equations (2.9), the second-order differential equations can be reduced to the first-order ones

$$
\begin{aligned}
&\Big(A_1 + \frac{1}{2}i\omega A_1\Big)e^{i\omega t} + \frac{1}{2i}\omega_1^2 A_1 e^{i\omega t} + \varepsilon\Big(\frac{1}{2}\lambda_1 A_1 e^{i\omega t} + \frac{\omega_1^2}{2i\omega}A_2 e^{i\omega t}\\
&\quad - \frac{\omega_1^2}{2i\omega}A_1 e^{i\omega t} - \frac{\alpha_1\omega_1^2}{8i\omega^3}A_1^3 e^{3i\omega t} + \frac{\alpha_1\omega_1^2}{8i\omega^3}|A_1|^2 A_1 e^{i\omega t} - \frac{f}{2}e^{i\omega t}\Big) + cc = 0\\
&\Big(A_2 + \frac{1}{2}i\omega A_2\Big)e^{i\omega t} + \frac{1}{2i}\omega_1^2 A_2 e^{i\omega t} + \frac{1}{2}\lambda_2 A_2 e^{i\omega t} - \frac{\alpha_2\omega_2^2}{8i\omega^3}A_2^3 e^{3i\omega t} + \frac{\alpha_2\omega_2^2}{8i\omega^3}|A_2|^2 A_2 e^{i\omega t}\\
&\quad + \omega_1^2\Big(\frac{1}{2i\omega}A_1 e^{i\omega t} - \frac{1}{2i\omega}A_2 e^{i\omega t}\Big) + \omega_2^2\frac{1}{2i\omega}A_2 e^{i\omega t} + \varepsilon\Big(\frac{1}{2}\lambda_2 A_2 e^{i\omega t} + \frac{\omega_2^2}{2i\omega}A_2 e^{i\omega t}\\
&\quad - \frac{\alpha_2\omega_2^2}{8i\omega^3}A_2^3 e^{i\omega t} + \frac{\alpha_2\omega_2^2}{8i\omega^3}|A_2|^2 A_2 e^{i\omega t} + \frac{1}{2}\lambda_1 A_1 e^{i\omega t} + \omega_1^2\frac{1}{2i\omega}A_2 e^{i\omega t}\\
&\quad - \omega_1^2\frac{1}{2i\omega}A_1 e^{i\omega t} - \frac{\alpha_1\omega_1^2}{8i\omega^3}A_1^3 e^{3i\omega t} + \frac{\alpha_1\omega_1^2}{8i\omega^3}|A_1|^2 A_1 e^{i\omega t} - \frac{f}{2}e^{i\omega t}\Big) + cc = 0
\end{aligned}
\qquad (2.13)
$$

It is well known that the mass damper system has the maximum amplitude of the main structure around the excitation frequency and the main structure. This paper only focuses on the amplitude when the excitation frequency is close to the frequency of the main structure. Therefore, $\omega \approx \omega_1$ is set, and only the $\exp(i\omega t)$ term is retained, which is the long-term term and needs to be eliminated according to its triangular form. According to the above principle, equations (2.13) can be reduced to

$$
\begin{aligned}
&\Big(A_1 + \frac{1}{2}i\omega A_1\Big) + \frac{1}{2i}\omega_1^2 A_1 + \varepsilon\Big(\frac{1}{2}\lambda_1 A_1 + \frac{\omega_1^2}{2i\omega}A_2 - \frac{(\omega_1^2}{2i\omega}A_1 + \frac{\alpha_1\omega_1^2}{8i\omega^3}|A_1|^2 A_1 - \frac{f}{2}\Big) = 0\\
&\Big(A_2 + \frac{1}{2}i\omega A_2\Big) + \frac{1}{2i}\omega_1^2 A_2 + \frac{1}{2}\lambda_2 A_2 + \frac{\alpha_2\omega_2^2}{8i\omega^3}|A_2|^2 A_2 + \omega_1^2\Big(\frac{1}{2i\omega}A_1 - \frac{1}{2i\omega}A_2\Big)\\
&\quad + \omega_2^2\frac{1}{2i\omega}A_2 + \varepsilon\Big(\frac{1}{2}\lambda_2 A_2 + \frac{\omega_2^2}{2i\omega}A_2 + \frac{\alpha_2\omega_2^2}{8i\omega^3}|A_2|^2 A_2 + \frac{1}{2}\lambda_1 A_1\\
&\quad + \omega_1^2\frac{1}{2i\omega}A_2 - \omega_1^2\frac{1}{2i\omega}A_1 + \frac{\alpha_1\omega_1^2}{8i\omega^3}|A_1|^2 A_1 - \frac{f}{2}\Big) = 0
\end{aligned}
\qquad (2.14)
$$

If we set $\omega = \omega_1 + \varepsilon\sigma$ and keep the binomial theorem to a small quantity of the first order, the above equation can be reduced to

$$
\begin{aligned}
&\frac{1}{\omega} = \frac{1}{\omega_1 + \varepsilon\sigma} = \frac{1}{\omega_1} - \frac{\varepsilon\sigma}{\omega_1^2} + \frac{\varepsilon^2\sigma^2}{\omega_1^3} + \dots\\
&\frac{1}{\omega^3} = \frac{1}{(\omega_1 + \varepsilon\sigma)^3} = \frac{1}{\omega_1^3} - \frac{3\varepsilon\sigma}{\omega_1^4} + \dots
\end{aligned}
$$

$$\dot{A}_1 + \varepsilon\Big(i\sigma A_1 + \frac{1}{2}\lambda_1 A_1 - \frac{i\omega_1}{2}A_2 + \frac{i\omega_1}{2}A_1 - \frac{3i\alpha_1}{8\omega_1}|A_1|^2 A_1 - \frac{f}{2}\Big) = 0 \qquad (2.15)$$

$$\dot{A}_2 + \frac{1}{2}\lambda_2 A_2 - \frac{3\mathrm{i}\alpha_2\omega_2^2}{8\omega_1^3}|A_2|^2 A_2 - \frac{\mathrm{i}\omega_1}{2}A_1 + \frac{\mathrm{i}\omega_1}{2}A_2 - \frac{\mathrm{i}\omega_2^2}{2\omega_1}A_2$$

$$+ \varepsilon\Big(\mathrm{i}\sigma A_2 + \frac{9\mathrm{i}\alpha_2\omega_2^2\sigma}{8\omega_1^4}|A_2|^2 A_2 + \frac{\mathrm{i}\sigma A_1}{2} - \frac{\mathrm{i}\sigma A_2}{2} + \frac{\mathrm{i}\omega_2^2}{2\omega_1^2}\sigma A_2 + \frac{1}{2}\lambda_2 A_2 - \frac{\mathrm{i}\omega_2^2}{2\omega_1}A_2$$

$$- \frac{3\mathrm{i}\alpha_2\omega_2^2}{8\omega_1^3}|A_2|^2 A_2 + \frac{1}{2}\lambda_1 A_1 + \omega_1^2\frac{1}{2\mathrm{i}\omega}A_2 + \frac{\mathrm{i}\omega_1}{2}A_1 - \frac{3\mathrm{i}\alpha_1}{8\omega_1}|A_1|^2 A_1 - \frac{f}{2}\Big) = 0$$

For the subsequent use of the multi-scale method, equation $(2.15)_4$ can be written as

$$\dot{A}_2 + \varepsilon\delta\Big(\frac{1}{2}\lambda_2 A_2 - \frac{3\mathrm{i}\alpha_2\omega_2^2}{8\omega_1^3}|A_2|^2 A_2 - \frac{\mathrm{i}\omega_1}{2}A_1 + \frac{\mathrm{i}\omega_1}{2}A_2 - \frac{\mathrm{i}\omega_2^2}{2\omega_1}A_2\Big)$$

$$+ \varepsilon\Big(\mathrm{i}\sigma A_2 + \frac{9\mathrm{i}\alpha_2\omega_2^2\sigma}{8\omega_1^4}|A_2|^2 A_2 + \frac{\mathrm{i}\sigma A_1}{2} - \frac{\mathrm{i}\sigma A_2}{2} + \frac{\mathrm{i}\omega_2^2}{2\omega_1^2}\sigma A_2 + \frac{1}{2}\lambda_2 A_2 - \frac{\mathrm{i}\omega_2^2}{2\omega_1}A_2 \qquad (2.16)$$

$$- \frac{3\mathrm{i}\alpha_2\omega_2^2}{8\omega_1^3}|A_2|^2 A_2 + \frac{1}{2}\lambda_1 A_1 + \omega_1^2\frac{1}{2\mathrm{i}\omega}A_2 + \frac{\mathrm{i}\omega_1}{2}A_1 - \frac{3\mathrm{i}\alpha_1}{8\omega_1}|A_1|^2 A_1 - \frac{f}{2}\Big) = 0$$

In formula $(2.15)_2$, $\varepsilon\delta = 1$.

3.   Multi-scale method

The multi-scale expansion method of the above equations is as follows

$$T_0 = t \qquad\quad T_1 = \varepsilon t \qquad\quad \cdots$$

$$A_1 = A_{10} + \varepsilon A_{11} \qquad A_2 = A_{20} + \varepsilon A_{21} \qquad \frac{d}{dt} = D_0 + \varepsilon D_1 \qquad D_n = \frac{\partial}{\partial T_n} \qquad (3.1)$$

By substituting the above expressions of A_1, A_2 and the time derivative into equations $(2.15)_3$ and (2.16), the following differential equation can be obtained

$$(D_0 + \varepsilon D_1)(A_{10} + \varepsilon A_{11}) + \varepsilon\Big[\mathrm{i}\sigma(A_{10} + \varepsilon A_{11}) + \frac{1}{2}\lambda_1(A_{10} + \varepsilon A_{11}) - \frac{\mathrm{i}\omega_1}{2}(A_{20} + \varepsilon A_{21})$$

$$+ \frac{\mathrm{i}\omega_1}{2}(A_{10} + \varepsilon A_{11}) - \frac{3\mathrm{i}\alpha_1}{8\omega_1}|A_{10} + \varepsilon A_{11}|^2(A_{10} + \varepsilon A_{11}) - \frac{f}{2}\Big] = 0$$

$$\qquad\qquad\qquad\qquad\qquad\qquad\qquad\qquad\qquad\qquad\qquad\qquad\qquad\qquad\qquad (3.2)$$

$$(D_0 + \varepsilon D_1)(A_{20} + \varepsilon A_{21}) + \varepsilon\delta\Big[\frac{1}{2}\lambda_2(A_{20} + \varepsilon A_{21}) - \frac{3\mathrm{i}\alpha_2\omega_2^2}{8\omega_1^3}|A_{20} + \varepsilon A_{21}|^2(A_{20} + \varepsilon A_{21})$$

$$- \frac{\mathrm{i}\omega_1}{2}(A_{10} + \varepsilon A_{11}) + \frac{\mathrm{i}\omega_1}{2}(A_{20} + \varepsilon A_{21}) - \frac{\mathrm{i}\omega_2^2}{2\omega_1}(A_{20} + \varepsilon A_{21})\Big] = 0$$

If equations (3.2) are taken as polynomials of ε, the first and second order coefficients of ε can be derived as follows

$$\varepsilon^0: \qquad D_0 A_{10} = 0 \qquad\quad D_0 A_{20} = 0$$

$$\varepsilon^1: \qquad D_1 A_{10} + \mathrm{i}\sigma A_{10} + \frac{1}{2}\lambda_1 A_{10} - \frac{\mathrm{i}\omega_1}{2}A_{20} + \frac{\mathrm{i}\omega_1}{2}A_{10} - \frac{3\mathrm{i}\alpha_1}{8\omega_1}|A_{10}|^2 A_{10} - \frac{f}{2} = 0 \qquad (3.3)$$

and

$$D_1 A_{20} + \delta\Big(\frac{1}{2}\lambda_2 A_{20} - \frac{3\mathrm{i}\alpha_2\omega_2^2}{8\omega_1^3}|A_{20}|^2 A_{20} - \frac{\mathrm{i}\omega_1}{2}A_{10} + \frac{\mathrm{i}\omega_1}{2}A_{20} - \frac{\mathrm{i}\omega_2^2}{2\omega_1}A_{20}\Big) = 0 \qquad (3.4)$$

At present, the research on mass dampers mainly focuses on the steady state of vibration. In this study, if it is in the steady state, the derivative in equation $(3.3)_2$ and (3.4) is set to 0

$$\mathrm{i}\sigma A_{10} + \frac{1}{2}\lambda_1 A_{10} - \frac{\mathrm{i}\omega_1}{2}A_{20} + \frac{\mathrm{i}\omega_1}{2}A_{10} - \frac{3\mathrm{i}\alpha_1}{8\omega_1}|A_{10}|^2 A_{10} - \frac{f}{2} = 0$$

$$\frac{1}{2}\lambda_2 A_{20} - \frac{3\mathrm{i}\alpha_2\omega_2^2}{8\omega_1^3}|A_{20}|^2 A_{20} - \frac{\mathrm{i}\omega_1}{2}A_{10} + \frac{\mathrm{i}\omega_1}{2}A_{20} - \frac{\mathrm{i}\omega_2^2}{2\omega_1}A_{20} = 0$$

(3.5)

By expanding A_{10} and A_{20} into complex numbers

$$A_{10} = a_1(\cos b_1 + \mathrm{i}\sin b_1) \qquad A_{20} = a_2(\cos b_2 + \mathrm{i}\sin b_2)$$

(3.6)

substituting equation (3.6) into equations (3.5), separating the real and imaginary parts, and setting $\omega_1 = 1$ to facilitate further analysis and solution, we have

$$\lambda_1 a_1 + a_2\sin(b_2 - b_1) = f\cos b_1$$

$$(2\sigma + 1)a_1 - \frac{3\alpha_1 a_1^3}{4} - a_2\cos(b_2 - b_1) = -f\sin b_1$$

$$\lambda_2 a_2 = a_1\sin(b_2 - b_1)$$

$$\frac{3\alpha_2\omega_2^2 a_2^3}{4} + (\omega_2^2 - 1)a_2 = -a_1\cos(b_2 - b_1)$$

(3.7)

The trig function cancelling b_1 and b_2 is obtained, order $\sigma = 0$

$$[3\alpha_2\omega_2^2 a_2^3 + 4(\omega_2^2 - 1)a_2]^2 + 16\lambda_2^2 a_2^2 = 16a_1^2$$

$$\lambda_1^2 a_1^2 + a_2^2 + 2\lambda_1\lambda_2 a_2^2 + a_1^2\left(1 - \frac{3\alpha_1 a_1^2}{2} + \frac{9\alpha_1^2 a_1^4}{16}\right) - 2a_2\left(1 - \frac{3\alpha_1 a_1^2}{4}\right)\sqrt{a_1^2 - \lambda_2^2 a_2^2} = f^2$$

(3.8)

In order to verify the accuracy of the above approximate solution method, equations (2.5) and (3.8) have been substituted into examples and solved twice by a numerical method to obtain frequency-amplitude curves of generalized coordinates after coordinate transformation. Figure 2 shows that the two curves are very close to each other, meeting the requirements of subsequent analysis.
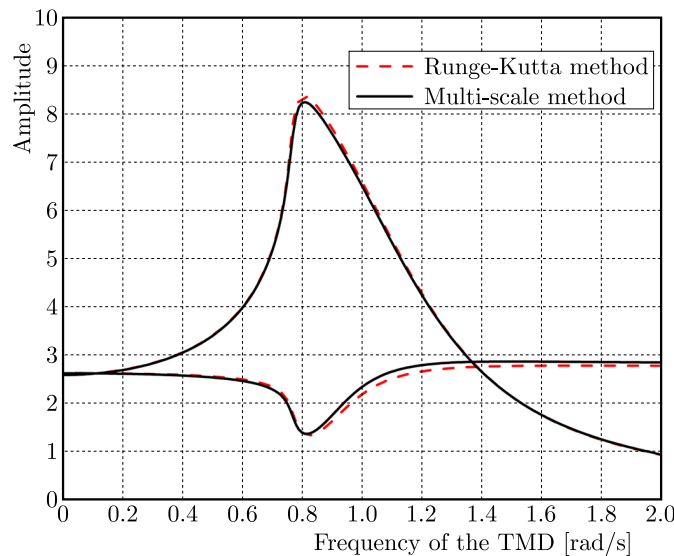

Fig. 2. Frequency-amplitude curve obtained using the Runge-Kutta method and the multi-scale method

4. Optimized frequency analysis of TMD

4.1. Algebraic equation of energy ratio

At different TMD frequencies, the amplitude is different, which leads to an optimal TMD frequency at which the amplitude of the main structure is minimum. In order to find the optimized frequency, it can be analyzed from the energy ratio. According to Eq. (2.3), x is approximately equal to displacement of the main structure, and y is the relative displacement of the main structure and the mass damper. In Fig. 2, the image of the peak line is the image of the amplitude of the relative displacement of the mass damper and the main structure changing with the frequency of the mass damper, and the image of the sunken line is the image of the amplitude of the main structure changing with the frequency of the mass damper. According to Fig. 2, when the amplitude of the relative displacement between the mass damper and the structure is maximum, the amplitude of the structure is minimum. According to the above conclusion, when the displacement amplitude of the main structure divided by the relative displacement amplitude is minimum, it is the optimal frequency. In short, the frequency at which the energy ratio E is the smallest, is the optimized frequency of the mass damper

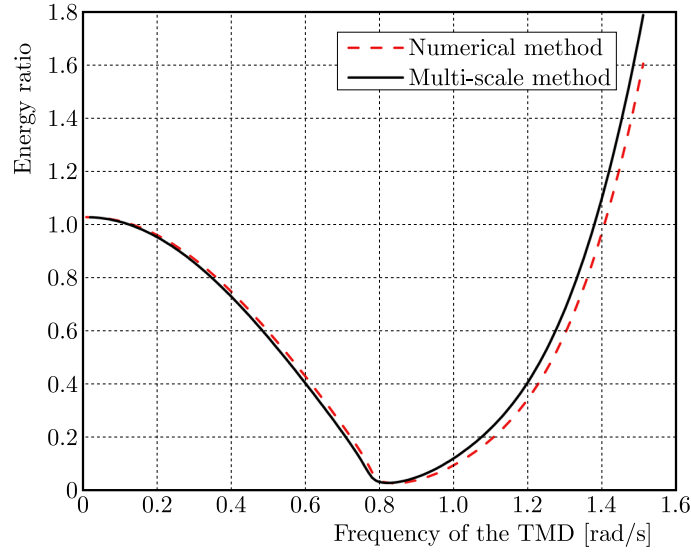$$E_1 = a_1^2 \qquad E_2 = a_2^2 \qquad E = \frac{a_1^2}{a_2^2} \tag{4.1}$$

Fig. 3. Frequency-energy ratio curve obtained using the numerical and multi-scale method

Figure 3 shows the change of energy ratio E caused by the change of mass damper frequency, and the selection of calculation example is the same as that in Fig. 2. By comparison, it can be seen that when the energy ratio E is the smallest, the displacement of the main structure is also the smallest, which confirms the accuracy of optimal frequency design using the energy ratio formula above. If the energy expressions are used for coordinate transformation of equations (3.8), the following expressions can be obtained

$$E_2^3 \frac{9\alpha_1^2 E^3}{16} + E_2^2 \left(-\frac{3\alpha_1 E^2}{2} + \frac{3\alpha_1 E}{2} \sqrt{E - \lambda_2^2} \right)$$
$$+ E_2 \left(\lambda_1^2 E + 1 + 2\lambda_1 \lambda_2 + E - 2\sqrt{E - \lambda_2^2} \right) - f^2 = 0 \tag{4.2}$$
$$\left[-\frac{3\alpha_2 \omega_2^2 E_2}{4} + (1 - \omega_2^2) \right]^2 = E - \lambda_2^2$$

4.2. Comparison between analytical solution and numerical method

This Section mainly checks the accuracy of the optimal frequency obtained according to the energy ratio design method by algebraic equations (4.2), and indirectly tests the accuracy of algebraic equations (3.8) obtained by this solution method. Of course, the solution time of algebraic equations is better than that of differential equations. Due to the limited space, it will not be described in detail in this paper. The accuracy is mainly compared with the TMD frequency of the minimum steady-state solution of the main structure obtained by solving differential equations (2.2) by the numerical method, so as to judge its accuracy. Because this paper mainly studies the structure with a small nonlinear coefficient, the response of the structure is in the steady-state stage, and there is no static bifurcation or jump phenomenon. It is verified that the response is independent of the initial conditions, so its steady-state response is the same under different initial conditions. The TMD frequency corresponding to the minimum steady-state response of the time history curve solved by the numerical method is compared with the optimal frequency obtained by the analytical method to verify the accuracy of this method. For $F = 0.3$ N, $\lambda_1 = 5$, $\lambda_2 = 0.16$, the excitation frequency and the main structure frequency are equal to 1. When $\alpha_1 = 0$ and $\alpha_1 = 1$ are compared, the optimal frequency variation of α_2 is from 0 to 0.01 as shown in Table 1 for the comparison of numerical and analytical solutions.

Table 1. Optimal frequency of the tuned mass damper, comparison between the numerical and analytical methods

α_1	α_2	Numerical solution	Analytical solution
0	0.000	1.006	1.000
	0.005	0.897	0.893
	0.010	0.817	0.818
	0.015	0.753	0.763
	0.020	0.703	0.720
1	0.000	0.999	1.000
	0.005	0.890	0.892
	0.010	0.809	0.817
	0.015	0.745	0.762
	0.020	0.696	0.719

The comparison results in the table show that when the excitation force is determined and the nonlinear coefficient is different, the error between the analytical solution and the simulation solution increases with an increase of the nonlinear coefficient, but the error is also very small. In the main research field of this paper, the nonlinear coefficient in practice is generally small, and the maximum error frequency is only 0.025, which meets the requirements of subsequent analysis.

4.3. TMD frequency design

A two-DOF system consisting of a main structure with cubic nonlinear stiffness and a non-linear TMD with cubic nonlinear stiffness is taken as the research object. The parameters of the structure are $m_1 = 1$ kg, $c_1 = 0.1$ Ns/m, $k_1 = 1$ N/m. The external load is a harmonic excitation, the excitation amplitude is $F = 0.3$ N, the excitation frequency is $\omega = 1$. As shown in Equations (2.3), the parameters are found according to the optimization method of the linear TMD. The mass ratio is $\varepsilon = 0.02$, so the parameters of TMD can be expressed as $\lambda_1 = 5$, $\lambda_2 = 0.16$. Because TMD in practice may produce nonlinear factors, large displacement and the existence of a limit device, the structure and quality of the linear damper are likely to produce nonlinear effects.

This article explores the structure itself due to the actual project of a nonlinear mass damper and determines optimal parameters with the influence of nonlinear stiffness for α_1 and α_2.

As shown in Fig. 4, when the nonlinear parameters of the mass damper increase, the optimal frequency decreases, which is shown on the left in the graph. At the same time, there is a more obvious change near the optimal frequency, which is shown to be steeper in the graph. When $\alpha_2 = 0.03$, that is when the cubic nonlinear stiffness of the mass damper is 3% of the linear stiffness value, the optimal frequency ω_{2opt} shifts from 1 to 0.65, which is a very large deviation and has a great influence on the vibration of the structure.
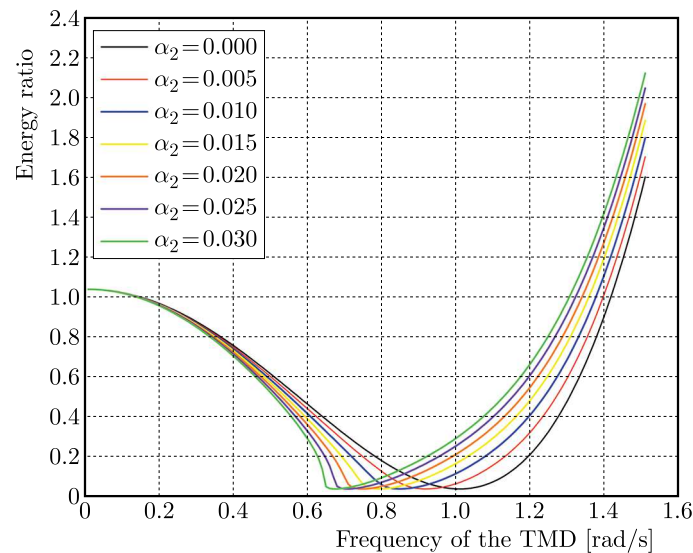

Fig. 4. Frequency-energy ratio curve obtained using the multi-scale method ($F = 0.3\,\mathrm{N}$, $\alpha_1 = 0.5$)

A linear design refers to the design of nonlinear structures by using the traditional linear method without considering nonlinear parameters of the tuned mass damper and the structure. Nonlinear design refers to consideration of nonlinear parameters $\alpha_1 = 0.5$, $\alpha_2 = 0.03$ by using equations (4.2) to find the optimal frequency. In linear design, the optimal frequency is $\omega_{2opt} = 1$.
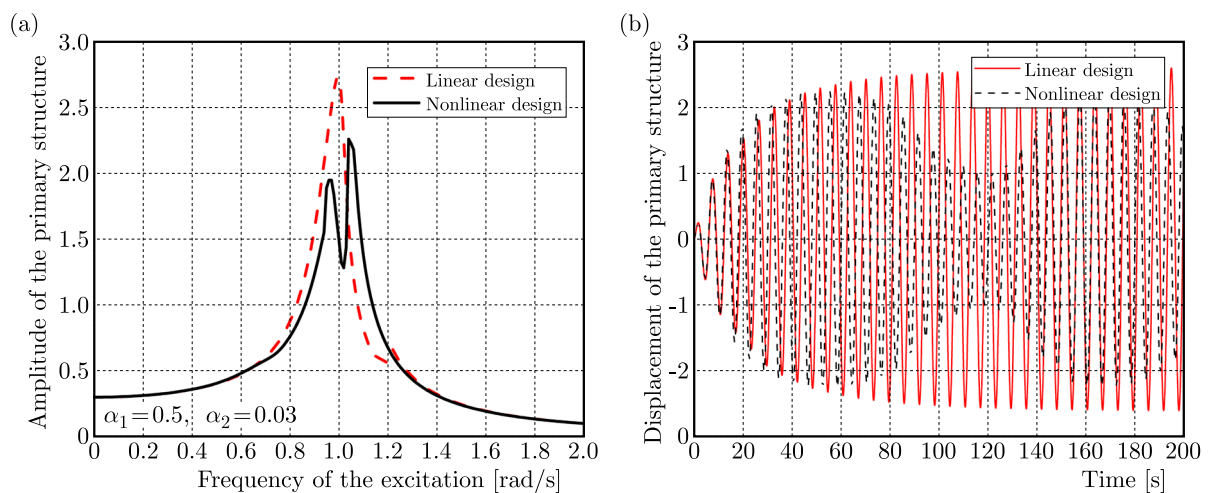

Fig. 5. Linear and nonlinear design ($F = 0.3\,\mathrm{N}$, $\alpha_1 = 0.5$, $\alpha_2 = 0.03$): (a) frequency of excitation-amplitude curves using the multi-scale method, (b) time history curves obtained using the numerical method

Figure 5a shows that the maximum displacement is achieved at the excitation frequency $\omega = 1.01$. If the nonlinear design is adopted, the optimal frequency is $\omega_{2opt} = 0.65$, and the

maximum displacement is obtained at $\omega = 1.05$. The time history diagram of the above main structure at the excitation frequency of its maximum displacement can be drawn, as shown in Fig. 5b. The above results show that there is a large deviation between the optimal frequency of the linear design and the nonlinear one $\omega_{2opt} = 1 \to 0.65$, and the nonlinear design effect is good.

Some papers have studied nonlinearity of tuned mass dampers, but few people considered the nonlinearity of both structure and mass dampers. In this paper, it is found that when the nonlinear parameter of the mass damper is zero, that is $\alpha_2 = 0$, it can be seen from equation $(4.2)_2$ that the energy ratio E is only related to the frequency of the mass damper and gets the minimum value at $\omega_2 = 1$. When the nonlinearity of the mass damper exists, it is difficult to see the influence from the equation alone, which can be further studied by using numerical examples. The nonlinear parameters of one structure are $\alpha_1 = 1$, $\alpha_2 = 0.02$, and those of the other structure are $\alpha_1 = 1$, $\alpha_2 = 0.02$ with the same other parameters. It can be seen from Fig. 5a that the optimal frequency has a certain deviation. Specifically, the optimal frequency offset is $\omega_{2opt} = 0.59 \to 0.66$, that is, the nonlinearity of the mass damper decreases the optimal frequency, while the nonlinearity of the structure increases the optimal frequency. Figure 5b shows a comparison between the above example without considering the structural nonlinearity and when the excitation frequency changes. According to Fig. 6c, the two curves are the time
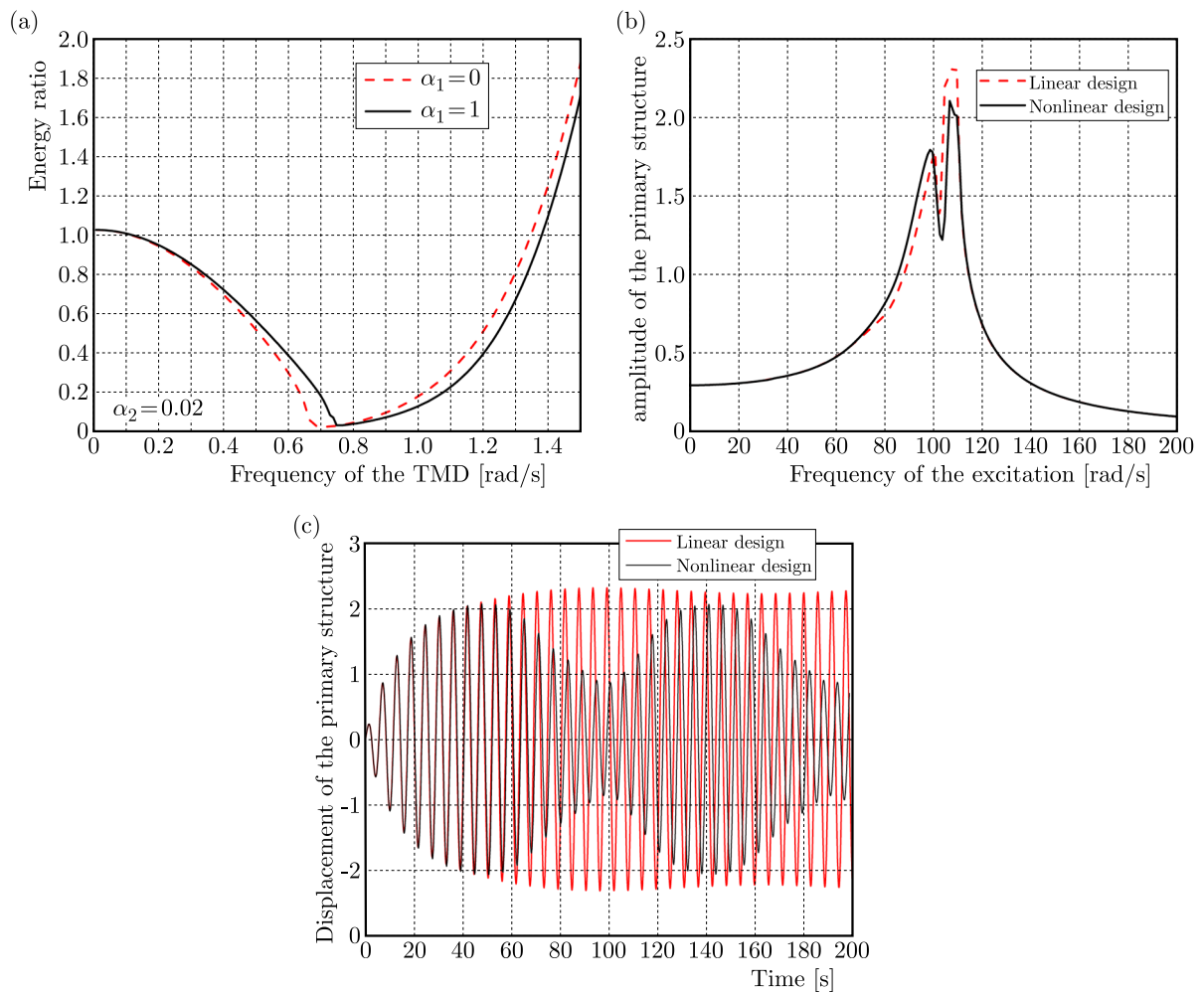

Fig. 6. Linear and nonlinear design ($F = 0.3$ N, $\alpha_2 = 0.02$): (a) frequency-energy ratio curve obtained by using the numerical method, (b) frequency of excitation-amplitude curves found using the multi-scale method, (c) time history curves obtained by using the numerical method

history curves under the excitation frequency of the maximum amplitude, respectively. It is not difficult to see that the structure has a good optimization effect after considering the nonlinearity of the structure.

As shown in Fig. 7, under different excitation frequencies, there is a maximum value of resonance for the main structure. When only the maximum amplitude of the main structure is compared, the linear mass damper with linear design has the best damping effect. As shown in Fig. 7, the yellow line represents the result without considering the nonlinearity of the mass damper, that is, the frequency diagram obtained for the optimal parameters of the linear mass damper. This is the vibration reduction effect of the mass damper in the ideal state. In practical engineering, the nonlinearity of mass dampers is an inevitable parameter. If the linear design is used to produce a nonlinear mass damper, which is indicated by the red dotted line in the figure, the vibration reduction effect is the worst, however notceable. If parametric design equations (4.2) are used for nonlinear design of the above nonlinear structure, the results obtained are better than those obtained by the linear design, but the desired damping effect of the linear mass damper is not achieved. The results of the above design are obtained under the condition that other parameters are determined, and only the excitation frequency changes and the nonlinearity of the mass damper exists. If the changes of other parameters are considered, the mass damper may have more optimized effects. In some experiments, it was found that the mass damper could not reach the expected effect, that is, the nonlinearity of the structure and the mass damper was not considered.
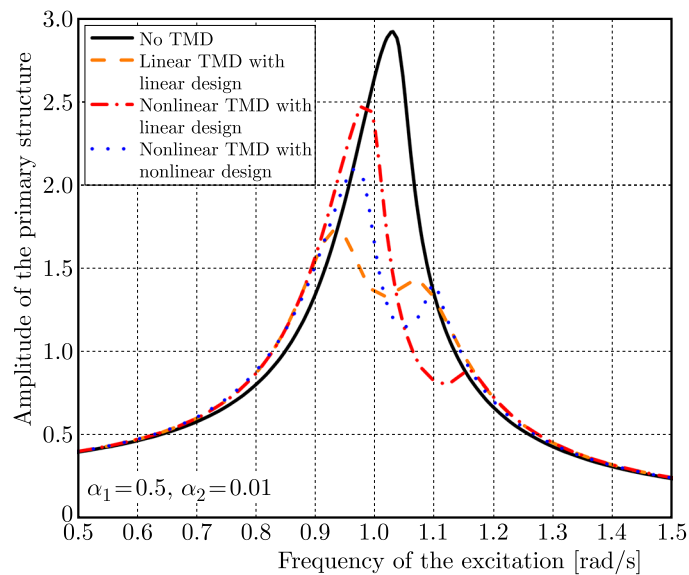

Fig. 7. Frequency of the excitation-amplitude of the primary structure curve
($F = 0.3$, $\alpha_1 = 0.5$, $\alpha_2 = 0.01$)

As shown in Fig. 8, the time-history curve shows intuitively that applying NTMD, whether linear or nonlinear design is used, can effectively reduce the displacement and acceleration of the steady-state response and transient response of the main structure. In this case, at the beginning of its transient response, the uncontrolled structure, the improved design and the linear design have the same response. In the subsequent steady-state response, the amplitude of the improved design is about 50% of that of the uncontrolled structure, and the amplitude of the linear design is about 70% of that of the uncontrolled main structure.
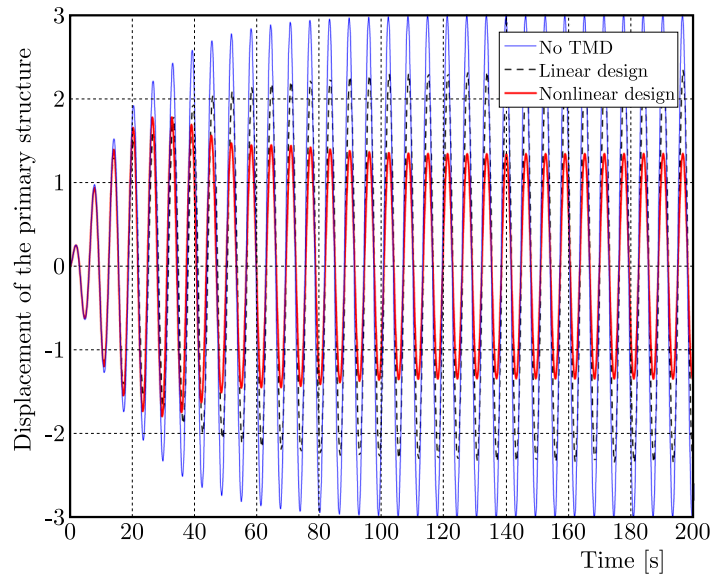
Fig. 8. Time-displacement curve using no TMD, linear and nonlinear design
($F = 0.3$, $\alpha_1 = 0.5$, $\alpha_2 = 0.01$)

5. Conclusion

In this paper, the nonlinear main structure and the nonlinear mass damper are studied. Taylor's expansion is used to decouple the equation of motion, and then the first order differential form of the equation is obtained by using the variational parameter method and the averaging method. Finally, the multi-scale method is used to solve the equations, and nonlinear equations for the amplitude and frequency are obtained. The equation obtained is formally valid for $\varepsilon \to 0$, but it needs to be used with care when mass dampers are used in systems with higher mass of the primary structure, because of mixing of the fast and slow time scales. Nevertheless, the method can be used to qualitatively evaluate at least some nonlinear mass damper systems. The conclusions are as follows:

- The results of solving the nonlinear equations obtained by the multi-scale method are compared with the results of solving the original two-degree-of-freedom second-order differential equations by the numerical method, and the error is small. The accuracy of the method is verified.
- The results show that the linear design formula has a poor effect on the design of nonlinear mass dampers, and the approximate optimization design formula based on energy has a better effect on the frequency findings of nonlinear mass dampers.
- The results show that if nonlinearity of the mass damper does not exist, the nonlinearity of the structure does not affect the change of the optimal frequency. If the mass damper nonlinearity exists, the structure nonlinearity will cause a change of the optimal frequency.

Improvement and exploration: This paper mainly explores the steady-state response for small nonlinear coefficients. The differential equations have stable solutions under variable initial conditions. In the case of a large nonlinear coefficient, in a certain TMD frequency range, the response will jump under different initial conditions, and the stability and sensitivity analysis must also be carried out. Due to the limited space of this paper, the above analysis process will be studied and discussed in the next paper.

References

1. ALEXANDER N.A., SCHILDER F., 2009, Exploring the performance of a nonlinear tuned mass damper, *Journal of Sound and Vibration*, **319**, 1-2, 445-462

2. ALMAZÁN J.L., DE LA LLERA J., INAUDI J.A., LÓPEZ-GARCIA D., IZQUIERDO L.E., 2007, A bidirectional and homogeneous tuned mass damper: A new device for passive control of vibrations, *Engineering Structures*, **29**, 7, 1548-1560

3. BADAMCHI K., KHALILI M.K., BADAMCHI K., 2021, Investigation of new proposed model for mass damper with geometrically nonlinear stiffness, *Journal of Structural and Construction Engineering*, **8**, 5, 163-178

4. BANERJEE S., GHOSH A., MATSAGAR V.A., 2022, Optimum design of nonlinear tuned mass damper for dynamic response control under earthquake and wind excitations, *Structural Control and Health Monitoring*, **29**, 7

5. BHOWMIK K., DEBNATH N., 2022, Stochastic design of multiple tuned mass damper system under seismic excitation, *Archive of Applied Mechanics*, **92**, 1, 383-404

6. DEN HARTOG J.P., 1956, *Mechanical Vibrations*, 4th Ed., Graw-Hill, New York

7. ELIAS S., MATSAGAR V., 2017, Research developments in vibration control of structures using passive tuned mass dampers, *Annual Reviews in Control*, **44**, 129-156

8. FARSHI B., ASSADI A., 2011, Development of a chaotic nonlinear tuned mass damper for optimal vibration response, *Communications in Nonlinear Science and Numerical Simulation*, **16**, 11, 4514-4523

9. FRAHM H., 1911, *Device for Damping Vibrations of Bodies*, U.S. Patent No. 989958

10. HOUSNER G.W., BERGMAN L.A., CAUGHEY T.K., CHASSIAKOS A.G., CLAUS R.O., MASRI S.F., SKELTON R.E., SOONG T.T., SPENCER B.F., YAO J.T.P., 1997, Structural control: past, present, and future, *Journal of Engineering Mechanics*, **123**, 9, 897-971

11. JIANG X.A., MCFARLAND D.M., BERGMAN L.A, VAKAKIS A.F., 2003, Steady state passive nonlinear energy pumping in coupled oscillators: theoretical and experimental results, *Nonlinear Dynamics*, **33**, 1, 87-102

12. KECIK K., MITURA A., 2020, Energy recovery from a pendulum tuned mass damper with two independent harvesting sources, *International Journal of Mechanical Sciences*, **174**, 105568

13. KIM S.Y., LEE C.H., 2020, Analysis and optimization of multiple tuned mass dampers with Coulomb dry friction, *Engineering Structures*, **209**, 110011

14. LI B.W., DAI K.S., MENG J.Y., LIU K., WANG J.Z., TESFAMARIAM S., 2020, Simplified design procedure for nonconventional multiple tuned mass damper and experimental validation, *The Structural Design of Tall and Special Buildings*, **30**, 2, e1818

15. LI L.Y., ZHANG T., 2020, Analytical analysis for the design of nonlinear tuned mass damper, *Journal of Vibration and Control*, **26**, 9-10, 646-658

16. LIAN J.J., ZHAO Y., LIAN C., WANG H., DONG X., JIANG Q., ZHOU H., JIANG J., 2018, Application of an eddy current-tuned mass damper to vibration mitigation of offshore wind turbines, *Energies*, **11**, 12, 3319

17. LIN G.L., LIN C.C., CHEN B.C., SOONG T.T., 2015, Vibration control performance of tuned mass dampers with resettable variable stiffness, *Engineering Structures*, **83**, 187-197

18. Lu Z., Wang Z.X., Zhou Y., Lu X.L., 2018, Nonlinear dissipative devices in structural vibration control: A review, *Journal of Sound and Vibration*, **423**, 18-49

19. Manevitch L.I., Gourdon E., Lamarque C.H., 2007, Parameters optimization for energy pumping in strongly nonhomogeneous 2 dof system, *Chaos Solitons and Fractals*, **31**, 4, 900-911

20. Matin A., Elias S., Matsagar V., 2020, Distributed multiple tuned mass dampers for seismic response control in bridges, *Proceedings of the Institution of Civil Engineers – Structures and Buildings*, **173**, 3, 217-234

21. Natsiavas S., 1992, Steady state oscillations and stability of non-linear dynamic vibration absorbers, *Journal of Sound and Vibration*, **156**, 2, 227-245

22. Nayfeh A.H., Mook A.D., 1981, *Nonlinear Oscillations*, Clarendon, Texas

23. Ormondroyd J., Den Hartog J., 1928, The theory of the dynamic vibration absorber, *Transactions of the American Society of Mechanical Engineers*, **50**, A9-A22

24. Qiu D., Seguy S., Paredes M., 2018, Design criteria for optimally tuned vibro-impact nonlinear energy sink, *Journal of Sound and Vibration*, **442**, 497-513

25. Ramlan R., Brennan M.J., Mace B.R., Kovacic I., 2010, Potential benefits of a non-linear stiffness in an energy harvesting device, *Nonlinear Dynamics*, **59**, 4, 545-558

26. Roberson R.E., 1952, Synthesis of a nonlinear dynamic vibration absorber, *Journal of the Franklin Institute*, **254**, 3, 205-220

27. Tai W.C., 2020, Optimum design of a new tuned inerter-torsional-mass-damper passive vibration control for stochastically motion-excited structures, *Journal of Vibration and Acoustics*, **142**, 1, 011015

28. Tsai H.-C., Lin G.-C., 1993, Optimum tuned-mass dampers for minimizing steady-state response of support-excited and damped systems, *Earthquake Engineering and Structural Dynamics*, **22**, 11, 957-973

29. Warburton G., Ayorinde E., 1980, Optimum absorber parameters for simple systems, *Earthquake Engineering and Structural Dynamics*, **8**, 197-217

30. Zhang X., Han Q., Bi K.M., Du X.L., 2022, An improved multi-mode seismic vibration control method using multiple tuned mass dampers, *Advances in Structural Engineering*, **25**, 4, 804-819

31. Zhao D., Du M., Ni T., Gong M., Ma L., 2020, Dual adaptive robust control for uncertain nonlinear active suspension systems actuated by asymmetric electrohydraulic actuators, *Journal of Low Frequency Noise Vibration and Active Control*, **40**, 3, 1607-1632